A Device for the Simultaneous Determination of the Water Retention Properties and the Hydraulic Conductivity Function of an Unsaturated Coarse Material; Application to a Green-Roof Volcanic Substrate

Filip Stanić, Yu-Jun Cui, Pierre Delage, Emmanuel de Laure, Pierre-Antoine Versini, Daniel Schertzer, Ioulia Tchiguirinskaia

A device for the simultaneous determination of the water retention properties and the hydraulic conductivity function of an unsaturated coarse material; application to a green-roof volcanic substrate

Filip STANIĆ[1,2], Yu-Jun CUI[1], Pierre DELAGE[1], Emmanuel DE LAURE[1], Pierre-Antoine VERSINI[2], Daniel SCHERTZER[2], Ioulia TCHIGUIRINSKAIA[2]

[1] Ecole des Ponts ParisTech, Navier/CERMES, Marne la Vallée, France

[2] Ecole des Ponts ParisTech, HM&Co, Marne la Vallée, France

Corresponding author:

Prof. Pierre Delage

Ecole des Ponts ParisTech

6-8 av. Blaise Pascal, Cité Descartes, Champs-sur-Marne

77455 Marne-la-Vallée cedex 2

France

Email: pierre.delage@enpc.fr

Phone: +33 1 64 15 35 50

Fax: +33 1 64 15 35 6

Abstract

The determination of the water retention curve (WRC) and the hydraulic conductivity function (HCF) of a specific volcanic coarse granular material used as a substrate for urban green roofs in Europe was carried out on a newly developed specific device in which low suctions, typical of coarse granular materials, were controlled. Smaller suctions (up to 32 *kPa*) were imposed by using a hanging column system and larger suctions (between 32 and 50 *kPa*) were imposed by using the axis translation technique in the same cell. The changes in suction during the tests were monitored by using a high accuracy differential pressure transducer. They were also used to determine the hydraulic conductivity function by means of both Kunze and Kirkham and Gardner's method. The former technique was used at low suctions (< 4 *kPa*) to account for the impedance effects due to the high air entry value ceramic porous disk and the latter was used between 4 and 50 *kPa*. Good comparability was observed in the data from both methods, demonstrating the good performance of the device. The mathematical expressions of the water retention curve of van Genuchten and Brooks and Corey were used, and a good fitting with our experimental data was obtained. Conversely, the hydraulic conductivity functions derived from these expressions appeared to lead to a significant under-estimation, confirming the need of operational and simple device for the experimental determination of the HCF. Also, this material proved to be an appropriate material for green urban infrastructures, due to light weight, satisfactory water retention capability and hydraulic conductivity.

Key words: Green-roof material; water retention; hydraulic conductivity; hanging column; axis translation; Gardner's method; Kunze and Kirkham's method

1. Introduction

Within the context of global warming, green roofs are considered as an efficient option to reduce the urban heat island (UHI) effect that characterizes large contemporary urban concentrations, thanks to the evapo-transpiration of the vegetal (lawn or trees) grown on them. Green roofs are also interesting to reduce urban run-off. The substrates used in green roofs have to be light enough and to present satisfactory water retention and transfer properties. Volcanic granular substrates appear to be relevant in this context, and they are frequently used in green roofs, like for instance in the case of the "Green Wave" of the Bienvenüe building (Versini et al. 2017) located close to Ecole des Ponts ParisTech in the Descartes campus of Marne la Vallée, 18 km east of Paris (*Figure 1*). The green roof is covering three waves or 260 *m* length and 80 *m* wide, on which a 20 *cm* thick layer of substrate has been placed. Actually, the use of substrates in urban green roofs appears to be rather empirical to date, and very little data on their water retention and transfer properties are available.

In this context, the paper describes the development and use of a specific controlled suction device, based on both a tensiometry principle, through the hanging column technique, and the axis translation method. The device is used to determine the water retention and transfer properties of a volcanic substrate (VulkaTec Riebensahm GmbH 2016, Germany; www.vulkatec.de) used in the Green Wave roof presented in *Figure 1*. Tensiometry controlled suction was applied by means of the hanging column technique by connecting a tube to a ceramic porous stone of 50 *kPa* air entry value on which a sample placed, and by imposing in the tube a water level lower than that of the sample. The axis translation method was implemented by using by applying air pressure on the top of the sample. The device was also used to determine the hydraulic conductivity function during the transient phases resulting from step increases in suction, by using the method proposed by Gardner (1956), accounting when necessary for the

impedance effects due to the permeability of the ceramic porous stone, by using Kunze and Kirkham (1962)'s method.

2. Material and methods

2.1. Material

The VulkaTec volcanic material is presented in the photo of *Figure 2* and its main characteristics are presented in *Table 1*. The material is very light with an average dry density of 1100 kg/m^3 so as not to load the roof significantly. A percentage of 4 % of organic matter was determined by using the French standard XPP94-047 1998, that consists in comparing the sample weight before and after heating during at least 3 hours at temperature between 450 and 500 °C. The grain size distribution curve of the substrate, determined by sieving following the French standard NFP94-056 (1996) is presented in *Figure 3* (solid line). The distribution of fine particles (< 80 µm) was obtained by sedimentation according to French standard NFP94-057 (1992). It can be noticed that 50% of the grains are larger than 1.6 *mm* with 10 % particles between 10 and 20 *mm*, in the coarse range and 13 % fine particles smaller than 80 µm. Also represented in *Figure 3* (dashed curve) is the grain size distribution curve of the material used for the test, with all particles smaller than 6 *mm*. Particles larger than 6 *mm* were discarded because we used a 70 *mm* diameter cell. For the same volume, a specimen with large particles discarded will contain more small particles, resulting in a larger porosity, in more water retained at a given suction, and in a larger hydraulic conductivity. Given that the proportion of the coarse particles discarded is 20%, a rough estimation of the over-estimation could be between 10 and 20 %. In *Table 1* are also presented the curvature coefficient C_c ($C_c = (D_{30})^2/(D_{60} \times D_{10}) = 1.95$) and the uniformity

coefficient C_u ($C_u = D_{60}/D_{10} = 55$). According to ASTM D2487-00 (2000), the material can be regarded as well graded.

2.2. Methods of controlling suction

The various methods of controlling suction in soils include the hanging column technique (Buckingham 1907), the axis translation technique (Richards 1941, 1947), the osmotic technique (Zur 1966) and the vapour equilibrium technique (Esteban 1990). A detailed description of these techniques and of their adaptation in geotechnical testing can be found in Delage (2002), Vanapalli et al. (2008), Blatz et al. (2008), Delage and Cui (2008) and Fredlund et al. (2012).

Given that the volcanic substrate investigated here is granular with rather large grain sizes (see *Figure 2*), it was initially decided to use the hanging column technique, because of its simplicity to use and of its good accuracy in both the control of low suctions and the measurement of water exchanges. However, one realized during the preliminary tests that, at the largest height imposed in the hanging column technique (3.2 *m*, corresponding to a suction of 32 *kPa*), a significant amount of water still remained in the substrate. It was then decided to impose larger suctions by using the axis translation technique.

In both cases, tests were conducted on a 24 *mm* high specimen placed into a metal 70 *mm* diameter cylindrical cell, in contact at its bottom with a 50 *kPa* air entry value ceramic porous disk. A thin metal disk (2 *mm* thick) was placed on top of the sample, so as to monitor changes in height by means of a displacement sensor (Mitutoyo Brand).

The Hanging column technique

The implementation of the hanging column technique is presented in *Figure 4*. The cell is connected at its base through valve V2 to an outlet controlled by valve V3 and to a water reservoir through valve V1. The cell is also connected through a central tube to a mobile device that allows the imposition of water levels lower than that of the sample, so as to apply suctions defined by the difference in water level between the sample and the mobile part (up to 32 *kPa* at the maximum height of 3.2 *m*).

The mobile device contains a smaller inner glass tube of d_{inn} = 0.5 *cm* and larger outer glass tube of diameter d_{out} = 1.5 *cm*. The inner tube is connected to the sample while the differential pressure transducer is connecting the outer tube with the reference glass tube (*Figure 5*). This pressure transducer (0.1 *mm* accuracy in water height) is able to provide high frequency measurements that are necessary for the determination of the hydraulic conductivity function. A monitoring rate of 10 *s* was adopted, chosen small enough to capture the change in the capillary potential at small times through the change of the water level in the mobile device. This change is detected as the height difference between the water levels either in the inner (valve V4 opened) or the outer tube (valve V5 opened), and the water level in the reference tube used to indicate constant reference water level. Most tubes used in the set-up are semi-rigid tubes made up of polyamide, except that used in the mobile device (inner and outer tubes) and the reference tube that are made up of glass.

The determination of the WRC along the drying path was carried out as follows:

Saturating the whole system: before starting, all the system has to be saturated, particularly the tubes connected to the differential pressure transducer, because air bubbles in the tubes can result in misleading data. Saturation was done by placing the reservoir filled with demineralized de-

aired water above the sample (*Figure 4*) and by opening valves V1 and V2 to let water infiltrate the sample from the bottom to the top. Saturation was considered satisfactory when a thin layer of water was observed on the sample top. Note that, whereas this procedure was satisfactory to saturate the large inter-grains pores, the full saturation of the small pores existing within the fine fraction (13% < 80 μm) was less guaranteed. To improve saturation, the water circulation between the bottom and the top of the specimen was let during one night. Then, valves V1 and V2 were closed. Prior to running the test, the mobile device was placed in such a position that the top of the inner tube full of water was at the same level as the top of the sample, resulting in $h_k = 0$ (*Figure 4*). In order to check whether equilibrium was ensured, valve V2 (*Figure 4*) was opened. If there was no water movement in the inner tube, the experiment could start. Otherwise, the saturation procedure was repeated.

Imposing suction: two methods were used, according to the value of suction imposed.

i) At smaller suctions, starting from saturation, it was observed that suction increases mobilized a significant volume of extracted water. Suction was then imposed by closing valves V2 and V5, by filling the inner tube up to the top and by moving down the mobile device at a position corresponding to the required suction. The water levels in the reference and outer tubes were carefully adjusted at the starting level in both tubes (*Figure 5a*). The imposed suction was defined by the difference in height between the top of the sample and the water level at the top of the inner tube (h_k in *Figure 4*). Valves V2 and V5 were then opened, resulting in water being extracted from the sample under the effect of increased suction. The extracted volume of water (ΔV in *Figure 4*) flows from the top of the inner tube into the outer tube. It is monitored by the differential pressure transducer that measures the height difference between the water levels in the outer and reference tubes (ΔH_1 - *Figure 5a*). Once equilibrium is reached (after approximately

10 – 12 hours), a point on the WRC is obtained from the pair of values (θ_i, $h_{k,i}$) from the following equation:

$$\theta_i = \theta_{i-1} - \Delta V_i / V_{sample,(i-\frac{1}{2})} \quad (1)$$

where ΔV_i is the volume of water [L^3] extracted from the sample, $V_{sample,(i-\frac{1}{2})}$ the average sample volume [L^3] between the end and the start of the test, determined from the monitored changes in height of the sample and $\theta_i - \theta_{i-1}$ the difference in volumetric water content [-] between the end and the start of the test. Note however that the monitoring of the changes in sample height during the tests indicated very small changes smaller than 0.5 *mm* (2%) along the whole test made up of 13 step increases in suction. The changes in height during each step were hence neglected.

ii) At larger suctions, the quantity of extracted water appeared to be much smaller and the procedure was changed to improve accuracy. The initial water level in the inner tube was no longer imposed at its top, but adjusted (by means of valve V3) at a lower level, in such a way that overflow was avoided during water extraction from the sample. The changes in height in the inner tube were then directly measured by the differential pressure transducer by closing valve V5 and opening valve V4. The imposed suction was calculated at the end of the measurement from the difference in height between the final water level in the inner tube and the top of the sample (ΔH_2 - *Figure 5b*).

Before each new suction step, water levels in the outer (i) / inner (ii) and reference tubes were adjusted to the same level by opening the bypass valve (*Figure 5*), in order to reset the differential pressure transducer. Water levels in the outer (i) / inner (ii) and reference tubes were then set to the required initial levels by carefully using valve V3, in order to eliminate extra water through the outlet.

In this study, only the drying path was considered. But the apparatus can also be used along wetting paths, along the following steps:

W1. Setting the initial position: the initial position of the mobile part is at the lowest vertical level, i.e. the final position at highest suction reached during the drying path. The sample is hence capable to store more water, thus a higher change in water level is expected. The water level change is recorded in the outer tube while the inner tube is filled up with water to the top, and no longer used during the test. Initial water levels in the outer and reference tubes should be set at the top of the inner tube by opening valves V1, V4 and bypass and letting water flow over the top of the inner tube. After reaching the required position, all valves and bypass should be closed.

W2. Imposing suction: by opening valves V5 and V2, water from the outer tube enters the sample. The resulting decrease in water level in the outer tube is captured by the differential pressure transducer.

W3. Reaching equilibrium: once equilibrium is reached, suction is calculated as the height difference between the water level in the outer tube and the top of the sample. The corresponding water content is calculated like during the drying path, but with an opposite sign because water content is now increasing after each measurement ($\theta_i = \theta_{i-1} + \Delta V_i / \mathrm{V}_{\mathrm{sample},(\mathrm{i}-\frac{1}{2})}$).

W4. Decreasing suction: to impose a lower suction, the mobile device is elevated, the outer and reference tubes are filled again, as described in step W1, and the W2 procedure is repeated. When a smaller change in water level in the outer tube is expected (lower suctions, higher water content), the inner tube should be used, by closing valve V5 and using valve V4, unlike in step W2.

W5. Final state of the wetting path: in order to saturate the sample, the mobile device should be located at the initial position of the drying path with the water levels in the inner and reference

tubes corresponding to the sample top. In case of a difference in height between the level in the inner tube and the top of the sample (if h_k marked in *Figure 4* is higher than zero) after reaching equilibrium, the tubes should be refilled with water by opening valves V1, V4 and the bypass. After closing valve V1 and the bypass and opening valve V2, without changing the vertical position of mobile device, no water movement in the inner tube should occur. If this is not the case, it means that the sample is not fully saturated and the refilling procedure should be repeated.

As commented above, the hanging column technique was used for heights up to 3.2 *m* corresponding to a maximum suction of 32 *kPa*. For higher suctions, the axis translation technique was applied.

The axis translation technique

The axis translation technique was carried out by applying increasing air pressure on the top sample surface. To do so, a cap connected to the air pressure supply source was placed on the top of the cell, as indicated in *Figure 6*. Tests were carried out while keeping the sample and the mobile device at the same level, above the differential manometer in order to monitor the changes in height difference. The imposed suction was calculated as the difference between the air pressure applied on the sample's upper surface and the change of water level inside the inner tube.

Before each test, the water level in the inner tube should be put at the same level as the top of the sample, and some space should be left above the water level to allow for some level increase with no overflow during the measurement. Once the air pressure is imposed, valves V2 and V6 are simultaneously opened, resulting in an increase of the water level in the inner tube, until stabilization at equilibrium. The final suction is calculated as the difference between the applied

air pressure and the pressure corresponding to the water level increment in the inner tube, captured by the pressure transducer. The corresponding water content is calculated by using Equation (1). This methodology was applied for suctions up to 50 *kPa*, the air entry value of the ceramic disk used. Higher suctions could be obtained with higher pressure and a ceramic disk of higher air entry value.

2.3. Determination of the hydraulic conductivity function

Saturated state

The investigation on the hydraulic conductivity function (HCF) of the material started with the determination of the saturated one. To do so, the cell containing the sample was disconnected from the device and connected to a Mariotte's bottle filled with demineralized, de-aired water, so as to run a constant head permeability test. Once the sample was saturated, the position of the bottom of the thin tube that goes through the Mariotte's bottle was set in such a way that the difference in height between the bottom of the thin tube and the top surface of the sample represented the imposed water head $\Delta\Pi$ [L]. The water level in the Mariotte's bottle had always to be above the bottom of the thin tube, in order to ensure a constant imposed water head. By measuring the water level change in the Mariotte's bottle ΔH [L] and the time necessary for obtaining this change Δt [T], the flux q [L/T] can be calculated.

$$q_n = \frac{\Delta H_n}{\Delta t_n}\frac{A_{mariotte}}{A} \qquad n = 1, 2, 3 \qquad (2)$$

where $A_{Mariotte}$ is the cross-section area of the Mariotte's bottle, decreased by the area of the thin tube. The saturated hydraulic conductivity K_s is then calculated using Darcy's law.

$$K_{s,n} = \frac{q_n}{\Delta\Pi_n} H_{sample} \qquad n = 1, 2, 3 \qquad (3)$$

255 The procedure was repeated for three different imposed water heads (n = 1, 2, 3), that were
256 adjusted by changing the altitude of the bottom of the thin tube.
257
258 *Unsaturated states*
259 The various existing methods of measuring the hydraulic conductivity functions in unsaturated
260 have been described in various papers or textbooks including Masrouri et al. (2008) and Fredlund
261 et al. (2012). In steady state methods (Corey 1957, Klute 1972, Olsen et al. 1985, among others),
262 a constant flow is imposed in a specimen put under given values of controlled suction. These
263 methods are known to be rather long and tedious, due in particular to the need of very precisely
264 measuring tiny transient flows along rather long periods of time. Alternatively, transient methods,
265 in which the water outflow from the specimen submitted to suction steps is monitored (Gardner
266 1956, Miller and Elrick 1958, Kunze and Kirkham 1962), are known to be easier to perform, with
267 simpler equipment (Masrouri et al. 2008). For these reasons, transient methods were used in this
268 work.
269 The HCF was hence determined by applying suction steps and monitoring the resulting changes
270 in water content $V(t)$ with time until equilibration, by means of the differential pressure
271 transducer. It was planned to calculate the hydraulic conductivity of the specimen by using
272 Gardner's method (Gardner 1956). This method assumes that the change in suction for each step
273 is small, in such a way that the diffusion coefficient $D(h_k)$ can reasonably be considered constant
274 during the test:
275 $$D(h_k) = D = \frac{K(h_k)}{C(h_k)} = \frac{K(h_k)\Delta h_k}{\Delta\theta} \quad (4)$$
276 where $C(h_k)$ is the average slope of the WRC [L^{-1}] along the suction step corresponding to Δh_k
277 [L] and $K(h_k)$ is the hydraulic conductivity [L/T]. Based on the analytical solution of the diffusion

equation expressed in terms of a Fourier series, Gardner proposed an estimation of the water conductivity using the monitored volume $V(t)$ [L^3] of water extracted from the sample:

$$V(t) = V_\infty \left(1 - \frac{8}{\pi^2} \sum_{n=1,3,5,\dots}^{\infty} \frac{1}{n^2} e^{-\left(\frac{n}{2}\right)^2 \pi^2 \frac{t}{T}}\right) \quad (5)$$

$$T = \frac{{H_{sample}}^2 C(h_k)}{K(h_k)} = \frac{{H_{sample}}^2}{D} \quad (6)$$

where V_∞ is the total amount of water extracted during the suction step [L^3]. As commented above, we observed in this work that the sample height H_{sample} remained reasonably constant, we hence adopted $H_{sample} = 2.4\ cm$.

Gardner's method is based on the fact that only the first member (n = 1) of the Fourier series in Equation (5) can be taken into account as a reasonable approximate solution, acceptable after $t > t_{bound} = \frac{4{H_{sample}}^2}{3\pi^2 D}$. In such conditions, the equation corresponding to the first member of Equation (5) can be written as:

$$ln[V_\infty - V(t)] = ln\frac{8V_\infty}{\pi^2} - \pi^2 \frac{Dt}{4{H_{sample}}^2} \quad (7)$$

showing that the term $ln[V_\infty - V(t)]$ becomes a linear function of time t, with a slope depending on the diffusion coefficient D.

The hydraulic conductivity $K(h_k)$ can then be calculated using the following equation:

$$K(h_k) = \frac{D\Delta\theta}{\Delta h_k} \quad (8)$$

The experimental data obtained in this work indicated that Gardner's method is more relevant at higher suctions, in which i) less water exchanges occurred, ii) the condition of constant suction is ensured and iii) the assumption about a constant diffusion coefficient D is more satisfactorily fulfilled.

298 However, Gardner's method cannot be directly used when the saturated hydraulic conductivity of
299 the ceramic disk is smaller than that of the sample. Experimental data showed that this occurred
300 during the first steps at low suction from the saturated state, during which higher hydraulic
301 conductivity values are obtained. To cope with the cases in which impedance effects due to the
302 ceramic disk occur, the method proposed by Kunze and Kirkham (1962) was adopted.
303
304 *Kunze and Kirkham's method*
305 Kunze and Kirkham (1962) considered the solution of the consolidation equation applied for
306 various layers of soil with different hydraulic conductivities. Their solution is graphically
307 presented through various curves showing the changes in $V(t)/V_\infty$ with respect to the variable
308 $\lambda_1^2 Dt/H_{sample}^2$ (see *Figure 11*), in which the parameter λ_1 is the first solution of equation
309 $a\lambda_n = cot\lambda_n$ and a is the ratio between the impedance of the ceramic disk and that of the sample.
310 The various curves in *Figure 11* correspond to various values of parameter a.
311 In order to determine the hydraulic conductivity $K(h_k)$ of the sample, it is required to estimate
312 parameters a and λ_1, by fitting the experimental data (presented in the form $V(t) / V_\infty$ versus t)
313 with one of the theoretical curves. Kunze and Kirkham (1962) remarked that only a portion of the
314 experimental data corresponded to the theoretical curves, so they recommended to rather fit the
315 curves at small times, for which more accurate values of λ_1^2 are obtained. The choice of the
316 adequate theoretical curve provides the value of parameter a. It is then possible to determine the
317 corresponding parameter λ_1 from the table presented in the paper of Kunze and Kirkham (1962).
318 It is also necessary to graphically determine the reference time t_{RP} that corresponds to
319 $\lambda_1^2 Dt / H_{soil}^2 = 1$ (vertical arrow in *Figure 11*). Finally, the diffusion coefficient is calculated as
320 $D = H_{soil}^2 / \lambda_1^2 t_{RP}$ and the hydraulic conductivity as $K = D\Delta\theta / \Delta h_0$.
321

Another way to explore a possible impedance effect due to the ceramic porous disk is to apply Darcy's law to the flux going through the saturated ceramic disk, as follows:

$$h_{k,top} = h_k + \Delta z_s \frac{\Delta V}{\Delta t} \frac{1}{A_{cs} K_{cs}} \quad (9)$$

where $h_{k,top}$ is the suction [L] at the top of the ceramic disk, Δz_s its thickness [L], A_{cs} its cross section area [L^2] (7 cm diameter), and ΔV is the volume [L^3] extracted from the sample during the time interval Δt [T].

The change in suction at the top of the ceramic disk can hence be derived from the monitoring of the extracted water volume ΔV with respect to time. In the lack of any impedance effect, both suction values at top and bottom should be equal.

3. Experimental results

3.1. Water retention curve

Figure 7 shows the continuous monitoring of the changes in suction with both the hanging column technique (steps 1 to 10) and the axis translation technique (steps 11 to 13). The outer tube was used for steps 1 and 2 that mobilized larger water volumes (valve V4 closed, valve V5 opened, see *Figure 5a*), while the subsequent 11 steps (3 – 13) were made by using the inner tube (valve V4 opened, valve V5 closed, see *Figure 5b*). In the former case, the imposed suction remains constant (Figure 8*a*, solid line with squares – the dashed line with triangles will be commented later on), while in the latter case (3 - 13), the initial instantaneous drop in height Δh_0 (increase in suction) is followed by a slight progressive increase in height, corresponding to a slight decrease in suction (see for example steps *11 - 12* in *Figure 8b*).

The corresponding drying path of the WRC is presented in *Figure 9*, in which the changes in volumetric water content θ are plotted with respect to changes in suction. The curve evidences a significant decrease in water content for the initial steps at low suctions, with θ decreasing from the initial value of 0.45 down to 0.29 upon application of the first suction step of 2.1 *kPa*. The increment in volumetric water content progressively decreases afterwards, with a decrease in θ to 0.25 at a suction of 4.2 *kPa*. The curve finally becomes almost linear at suction larger than 14.2 *kPa*, indicating that the further suction increments extract small quantities of water. A final value of 0.16 is reached at 49.6 *kPa*. Good compatibility is observed between the section obtained with the hanging column technique (1 – 10) and that with the axis translation method (11 – 13).

Figure 9 also shows that a good fitting is obtained by using the WRC expressions of Brooks and Corey (1964) and van Genuchten (1980), as follows:

- van Genuchten (vG): $\theta = \theta_r + \frac{\theta_s - \theta_r}{[1+(\alpha h_k)^n]^m}$; with $m = 1 - \frac{1}{n}$ *(10)*

where θ_s is the saturated volumetric water content (θ_s = 0.45, see Figure 9), θ_r [-] the residual one, α = 1 / h_a [L^{-1}] where h_a [L] is the air entry value expressed in water height, and n [-] an empirical parameter;

- Brooks & Corey (BC): $\theta = \theta_r + (\theta_s - \theta_r)\left(\frac{h_k}{h_a}\right)^{-\lambda}$ *(11)*

where λ [-] is an empirical parameter.

The fitting of the parameters of both vG and BC curves were made by first adopting values of h_a and θ_r, taken equal to 3.2 cm and 0.11, respectively. The best fitting was obtained with n = 1.35 (vG expression) and λ = 0.35 (BC expression).

3.2. Hydraulic conductivity function

Saturated state

Figure 10 shows the data obtained from the steady-state permeability test, expressed in terms of changes in fluxes q_n with respect to the hydraulic gradient ($i = \Delta\Pi_n / H_{sample}$, see Equation 3). The slope of the linear regression corresponding to the three measured points (n = 1, 2, 3) and to point (0, 0) provides a value K_s = 8.11 x 10^{-6} *m/s*.

The same approach carried out on the ceramic porous stone provided a value K_{cs} = 4.02 x 10^{-8} *m/s*, confirming that the hydraulic conductivity of the saturated ceramic porous stone is significantly smaller than that of the saturated material. As a consequence, Kunze and Kirkham's method was used to interpret the data of the first suction steps (1 and 2) applied from the saturated state.

Unsaturated states

Figure 11 presents the experimental data of steps 1 and 2 presented in terms of changes in $V(t)/V_\infty$ with respect to a log scale of $\lambda_1^2 D t_{RP}/H_{sample}$, as proposed by Kunze and Kirkham. For step 1, *Figure 11* shows excellent agreement of the data with the theoretical curve of parameter a = 1. The corresponding value of parameter λ_1^2 is 0.74, according to Kunze and Kirkham (1962)'s graph, while the reference time t_{RP} is 47 *min* (2800 *s*). Finally, a hydraulic conductivity $K(s)$ = 2.14 x 10^{-7} *m/s* is obtained for a suction of 2.1 *kPa*. This value is larger than that of the ceramic disk (K_{cs} = 4.02 x 10^{-8} *m/s*), confirming the necessity of accounting for the impedance effect of the porous stone.

Similarly, a value a = 0.142 is obtained for step 2, with λ_1^2 = 1.90 with t_{RP} = 24 *min* (1440 *s*), resulting in a hydraulic conductivity value of 3.64 x 10^{-8} *m/s*, slightly smaller than that of the ceramic porous stone.

The calculations of the changes with time of the suction imposed on the top of the ceramic disk according to Equation 10 are presented in *Figure 8a* for step 1 and 2 (dashed line with triangles). As expected, they confirm the perturbation due to the low permeability of the ceramic disk. This perturbation is stronger during step 1, in which almost 3 hours are necessary to reach the desired 2.1 *kPa* suction at the top, compared to step 2 in which the 4.2 *kPa* imposed suction is reached at the top after less than 2 hours.

Prior to use Gardner's method, the assumption of constant suction during each suction step has to be checked. Inspection of the suction steps applied for suctions higher than 4.1 *kPa* (steps 3 – 13, *Figure 7)* showed that the water level in the inner tube was slightly rising at the start of the step, hence decreasing the suction. The level changes in the inner tube during steps 3 and 4 are around 7.5 % of the imposed suction and 30 % of the imposed suction increment. These two steps do not reasonably ensure the constant suction condition, they will not be considered for the determination of the HCF. For suctions higher than 10 *kPa* (measurements 5 – 13, *Figure 7*), the level increase in the tube is smaller (less than 4 % of the imposed suction and less than 12 % of the imposed suction increment), and suction changes are considered to be reasonably compatible with the use of Gardner's method (see for example steps 11 and 12 in *Figure 8b*).

The application of Gardner's method is presented in *Figure 12*, that shows the changes in $ln[V_\infty - V(t)]$ with respect to time for the measurements made during steps 2 and 5 – 13 (see Equation 7). In all cases, the linearity of the $ln[V_\infty - V(t)]$ function is satisfactory. As

411 recommended by Gardner, the fitting is only based on the points corresponding to $t > t_{bound}$. The
412 values of t_{bound}, calculated for each stage, are given in the graph of each step. Values are included
413 between 0.2 and 2 *h*, depending of the value of *D*. Note that step 2 was also considered here, so
414 as to compare the data with that of Kunze and Kirkham's method, that is more appropriate, given
415 possible impedance effects.
416
417 *Figure 13* shows the hydraulic conductivities obtained using the three different methods: i)
418 saturated hydraulic conductivity, using the constant-head permeability test, ii) unsaturated
419 hydraulic conductivity at lower suctions, using Kunze and Kirkham's method (steps 1 and 2) and
420 iii) unsaturated hydraulic conductivity at larger suctions, using Gardner's method (steps 2' and 5
421 to 13).
422
423 One observes that the hydraulic conductivity at step 2' provided by Gardner's method is
424 somewhat smaller than that (step 2) given by Kunze and Kirkham's method. This is compatible
425 with the impedance effect due to the low permeability of the ceramic disk, that indicates that
426 Gardner's method is not fully satisfactory for step 2. Note however that the difference in
427 hydraulic conductivity is not that large (3.64×10^{-8} m/s for Kunze and Kirkham and 1.64×10^{-8}
428 m/s for Gardner's method).
429
430 All the points obtained by the three methods are in reasonable agreement and provide the
431 decrease in hydraulic conductivity with increased suction along the drying path. In the first 5
432 steps, a large decrease of 4 orders of magnitude is observed from 10^{-5} m/s (saturated state) down
433 to 10^{-9} m/s at a suction of 10.4 *kPa*, and the hydraulic conductivity then stays between 10^{-9} and
434 10^{-10} m/s for steps 5 to 13, corresponding to suctions between 10.4 and 49.6 *kPa*.

The results are also compared with the curves obtained by using the mathematical expressions of the relative hydraulic conductivity ($K_r(h_k) = K(h_k) / K_s$) derived from the WRC formulations of Brooks and Corey (1964) and van Genuchten (1980) according to Mualem (1970)'s approach (Equations 10 and 11), as follows:

- van Genuchten: $K_r(h_k) = \frac{\{1-(\alpha h_k)^{n-1}[1+(\alpha h_k)^n]^{-m}\}^2}{[1+(\alpha h_k)^n]^{m/2}}$ *(12)*

- Brooks & Corey: $K_r(h_k) = \left(\frac{h_k}{h_a}\right)^{-2-5\lambda/2}$ *(13)*

The curves obtained with the parameters obtained from the WRC curves, also represented in *Figure 13*, do not satisfactorily fit with the experimental data. Both formulations underestimate the hydraulic conductivity, with a better correspondence observed with the Brooks and Corey formulation. Because of this poor correspondence, it was decided to propose a power law, fitted by using the root-mean-square-deviation (RMSD) method. This solution can be written in the following form:

$$K(s) = a_1 \times s^{b_1} \quad (14)$$

with a_1 = 5.38 x 10^{-7} and b_1 = - 2.283, giving:

$$K(s) = 5.38 \times 10^{-7} \times s^{-2.283} \quad (15)$$

The corresponding expression of the relative permeability is then:

$$\frac{K(s)}{K_s} = a_2 s^{b_1} = 6.63 \times 10^{-2} \times s^{-2.283} \quad (16)$$

In order to present the right side of Equation (16) in the relative form as well, coefficient a_2 can be written as follows:

$$a_2 = \left(\frac{1}{s_0}\right)^{b_1} \rightarrow s_0 = a_2^{-\frac{1}{b_1}} = 0.305 \quad (17)$$

where s_0 is the suction value corresponding to the air entry value, expressed in [*kPa*]. The final form of the equation reads:

$$\frac{K(s)}{K_s} = \left(\frac{s}{s_0}\right)^b \quad (18)$$

with s_0 = 0.305 *kPa* and $b = b_1$ = -2.283.

4. Conclusion

The new device developed in this work allowed to determine the water retention curve and the hydraulic conductivity function of a light coarse material used as substrate in an urban green roof. In a first estimation, it was estimated than the hanging column technique of controlling suction, with a maximum height of 3.2 *m* (suction 32 *kPa*) would have been satisfactory, but it was finally necessary to impose larger suctions by using the axis translation technique. This adaptation was rather simple to carry out, finally allowing to run the whole test by using both techniques on the same specimen in the same cell between the saturated state and a maximum suction of 49.6 *kPa*, with a good comparability between the experimental data obtained by the two techniques.

The advantage of the hanging column technique is to allow for a very good precision in the control of both the suction and the water exchanges, made possible by using a differential pressure sensor with an accuracy of 0.1 *mm* in height. A specific system based on the use of both an inner and an outer tube was also developed so as to improve the accuracy of the measurements along the range of the applied suctions. This good accuracy was necessary, given the significant changes in volumetric water content observed during the first application of a suction as low as 2.1 *kPa*, that resulted in a significant decrease from 0.45 to 0.29.

Starting from a saturated state, the WRC exhibited a drastic decrease under a small suction of 2.1 *kPa*, in link with the coarse nature of the granular substrate, followed by a progressive decrease down to a water content of 0.16 at 49.6 *kPa*. Both the van Genuchten and Brooks and Corey mathematical expressions fitted quite nicely with the experimental data.

The good accuracy in the measurements of suction and water exchanges also allowed to simultaneously determine, in a simple fashion, the hydraulic conductivity function from the monitoring of the water exchanges resulting from the step changes in suction. At lower suctions (2.1 and 4.2 *kPa*) and higher hydraulic conductivity, it was necessary to account for the impedance effects due to the 50 *kPa* air entry value ceramic disk by successfully using Kunze and Kirkham's method. Gardner's method was used at larger suctions, and a good comparability was observed from the experimental data from each technique. Another advantage of the device is to simply allow for the determination of both the water retention curve and the hydraulic conductivity function of the coarse material. Unsurprisingly, the HCF function exhibit a trend similar to that of the WRC, with a decrease of around 3 orders of magnitude between the saturated state and that at a suction of 4.2 *kPa*, whereas all the data between 10.4 and 49.6 *kPa* were comprised between 10^{-9} and 10^{-10} m/s.

The experimental HCF data were compared with the analytical expressions derived from the WRC expressions of van Genuchten and Brooks and Corey, based on Mualem's approach. In both cases, these expressions appeared to significantly underestimate the experimental HCF, with however better results with Brooks and Corey's expression, that was less than one order of magnitude below the experimental data. These expressions of the HCF are often used in the lack of experimental data, and the difference observed in this work confirm the need of having

operational devices for the simultaneous experimental determination of the water retention curve and the hydraulic conductivity function in granular materials such as the green roof substrate investigated in this work.

5. References

ASTM D2487-00: Standard Practice for Classification of Soils for Engineering Purposes (Unified Soil Classification System), *Annual Book of ASTM Standards*, ASTM International, West Conshohocken, PA, 2000.

Blatz, J., Cui, Y.-J., Oldecop, L.A., 2008, "Vapour equilibrium and osmotic technique for suction control," *Geotech. Geol. Eng*., doi:10.1007/s10706-008-9196-1

Brooks, R.H, Corey, A. T., 1964, "Hydraulic properties of porous media," *Hydrology papers*, No.3.

Corey, A.T., 1957, "Measurement of water and air permeability in unsaturated soil," *Soil Sci. Soc. Am. Proc.*, Vol. 21, No. 1, pp. 7–10.

Buckingham, E., 1907, "Studies on the movement of soil moisture," Bull 38 USDA, Bureau of Soils, Washington DC.

Cui, Y. J., Delage, P., Alzoghbi, P., 2003, "Retention and transport of a hydrocarbon in a silt," *Géotechnique*, Vol. 53, No. 1, pp. 83-91.

Delage, P., 2002, "Experimental unsaturated soil mechanics: State-of-art-report," 3rd International conference on unsaturated soils, Vol. 3, Recife.

Delage, P., Cui, Y.-J., 2008, "An evaluation of the osmotic technique of controlling suction,"

Geomech. Geoengin. Int. J., Vol. 3, No. 1, pp. 1–11.

Esteban, F., 1990, “Caracterización de la expansividad de una roca evaporítica. Identificación de los mecanismos de hinchamiento”, Tesis doctoral de la Universidad de Cantabria, Santander.

Fredlund, D. G., Rahardjo, H. and Fredlund M. D., 2012, *Unsaturated Soil Mechanics in Engineering practice*, Wiley, New York.

Fredlund, D. G., and Xing., A., 1994, "Equations for the soil-water characteristic curve," *Can. Geotech. J*, Vol. 31, pp. 521-532.

Gardner, W. R., 1956, "Calculation of Capillary Conductivity from Pressure Plate Outflow Data." *Soil Science Society Proceeding*, Vol. 20, pp. 317 - 320.

Klute, A., 1972, “The determination of the hydraulic conductivity and diffusivity of unsaturated soils,” *Soil Sci.*, Vol. 113, No. 4, pp. 264-276.

Kunze, R. J., and Kirkham, D., 1962, “Simplified Accounting for membrane impedance in Capillary Conductivity Determinations,” *Soil Sci. Soc. Am. Proc.*, Vol. 26, pp. 421-426.

Li, Y., and Babcock Jr., R. W., 2016, “A Simplified Model for Modular Green Roof Hydrologic Analysis and Design,” *Water*, Vol. 8, No. 343, pp. 1 – 13.

Masrouri, F., Bicalho, K.V., Kawai, K., 2008, “Hydraulic testing in unsaturated soils,” *Geotech. Geol. Eng.*, Vol. 26, pp. 691 – 704, doi:10.1007/ s10706-008-9202-7.

Miller, E., Elrick, D., 1958, “Dynamic determination of capillary conductivity extended for non-negligible membrane impedance,” *Soil Sci. Soc. Am. Proc.*, Vol. 22, pp. 483–486.

Mualem, Y., 1976, “A New Model for Predicting the Hydraulic Conductivity of Unsaturated Porous Media,” *Water Resources Research*, Vol. 12, No. 3, pp. 513-522.

NFP94-056, "Analyse granulométrique - Méthode par tamisage à sec après lavage," French Standard, AFNOR Editions, Paris La Défense Cedex, 1996.

NFP94-057, "Analyse granulométrique des sols - Méthode par sédimentation," French Standard, AFNOR Editions, Paris La Défanse Cedex, 1992.

Olsen, H.W., Nichols, R.W., Rice, T.L., 1985, "Low gradient permeability methods in a triaxial system," Géotechnique, Vol. 35, No. 2, pp. 145–157.

Richards, L.A., 1941, "A pressure-membrane extraction apparatus for soil solution," *Soil Sci*., Vol. 51, No. 5, pp. 377–386.

Richards, L.A., 1947, "Pressure-membrane apparatus – construction and use," *Agric. Eng*., Vol. 28, pp. 451–460.

Vanapalli, S.K., Sharma, R.S., Nicotera, M.V., 2008, "Axis-translation and negative water column techniques for suction control," *Geotech. Geol. Eng*., Vol. 26, pp. 645 – 660, doi:10.1007/ s10706-008-9206-3.

van Genuchten, M. Th., 1980, "A Closed-form Equation for Predicting the Hydraulic Conductivity of Unsaturated Soils," *Soil Sci. Soc. Am. J*, Vol. 44, pp. 892-898.

Versini, P.A., Gires, A., Fitton, G., Tchiguirinskaia, I., Schertzer, D., 2017, "La Vague Verte de l'ENPC: un site pilote de Blue Green Dream pour évaluer les variabilité spatio-temporelles du bilan hydrologique d'une infrastructure végétale - ENPC Blue Green Wave: a Blue Green Dream pilot site to assess spatio-temporal variability of hydrological components in green infrastructures," *La Houille Blanche*, Accepted for publication.

VulkaTec Riebensahm GmbH, "Assurance qualité - Vulkaplus intensiv 0-12," GUTEGEMEINSCHAFT SUBSTRATE FUR PFLANZEN E.V., Kretz, Germany, 2016.

XPP94-047, "Détermination de la teneur pondérale en matières organiques d'un matériau," French Standard, AFNOR Editions, Paris La Défanse Cedex, 1998.

Zur, B., 1966, “Osmotic control the matric soil water potential,” *Soil Sci.*, Vol. 102, pp. 394–398

Acknowledgements

The authors are indebted to the VulkaTec Riebensahm GmbH Company (Germany) for providing the substrate material investigated in this study. They are also grateful to the two anonymous reviewers for their comments, that helped improving the quality of the paper.

Table 1. Basic characteristics of "Green Wave" substrate

Dry density	Porosity	Curvature coefficient	Uniformity coefficient	Percentage of organic matter
ρ_s [kg/m^3]	n [-]	C_c [-]	C_u [-]	C_{MOC} [%]
1100	0.448	1.95	55	4

List of Figures

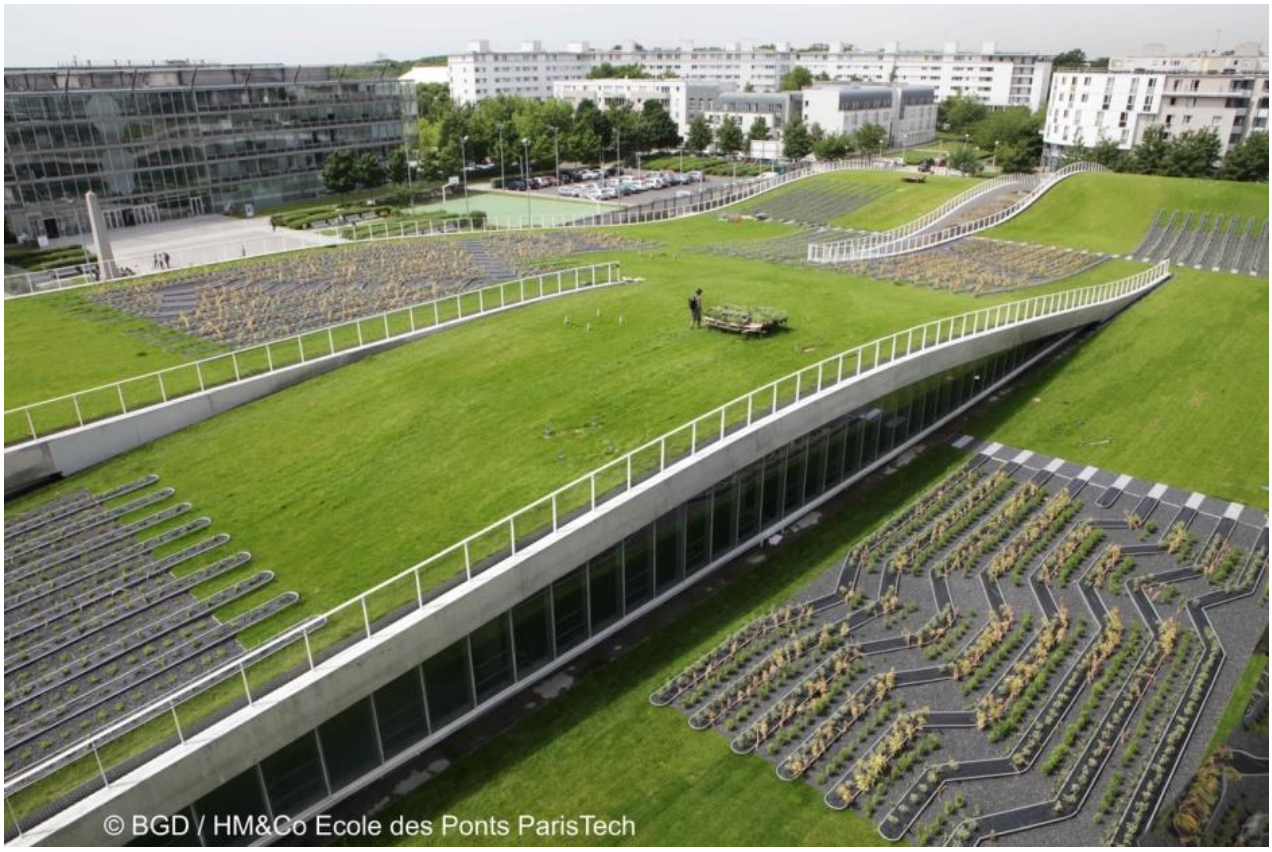

Figure 1. The "Green Wave" of the Bienvenüe building located close to Ecole des Ponts ParisTech, Marne la Vallée

Figure 2. Photo of the volcanic substrate used for the "Green Wave"

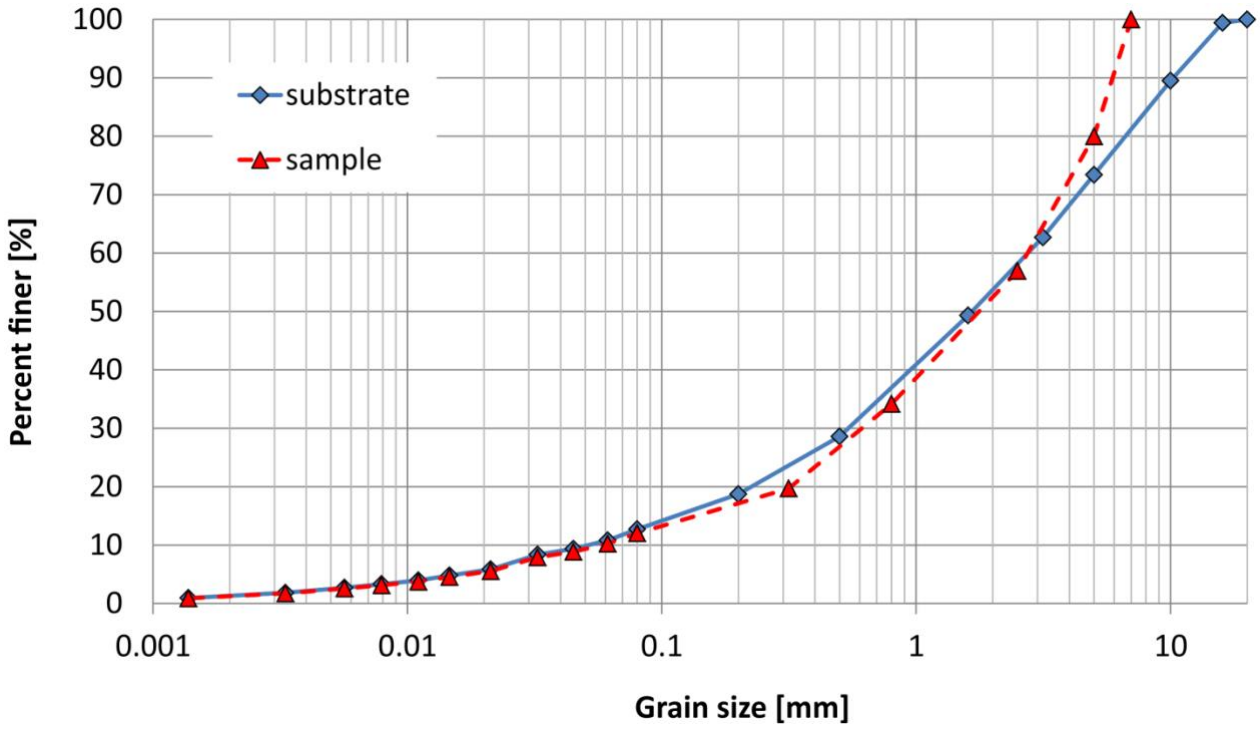

Figure 3. Grain size distribution curve of the volcanic substrate

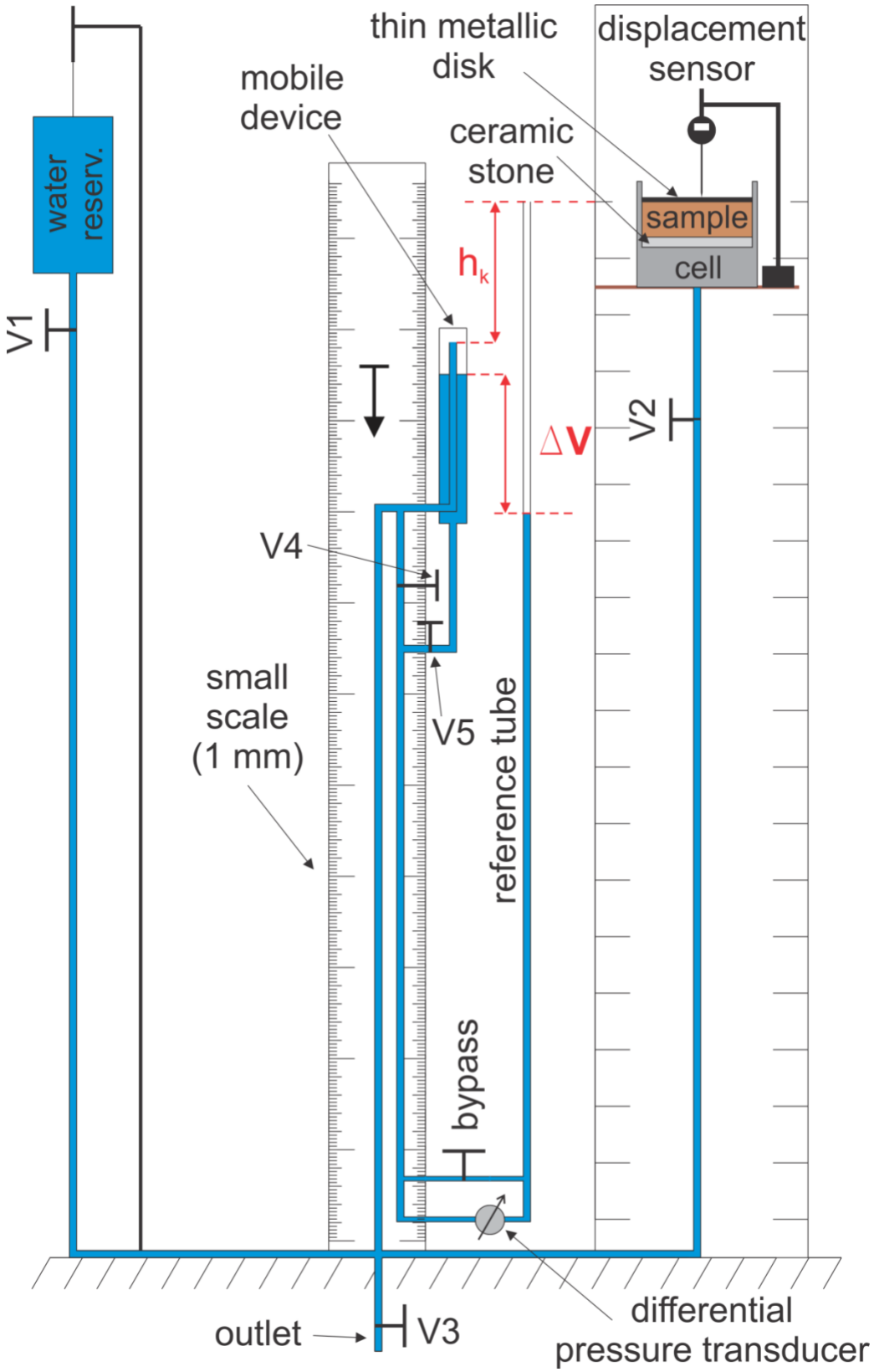

630

631 *Figure 4. General lay-out of the hanging column system*

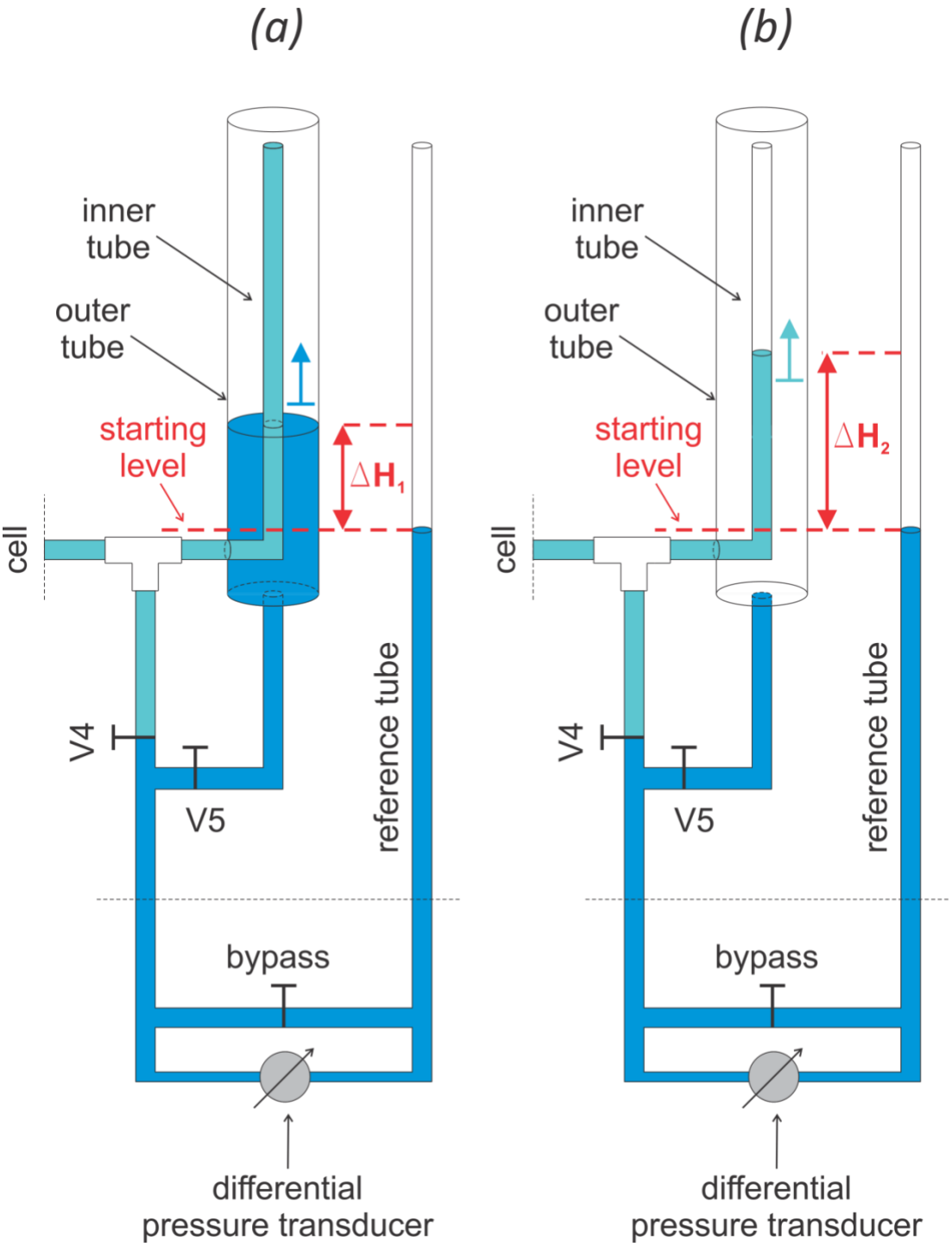

Figure 5. Description of the two procedures used: a) change in water level observed the in outer tube (ΔH_1) with valve V4 closed and valve 5 opened; b) change in water level observed in the inner tube (ΔH_2) with valve 4 opened and valve 5 closed.

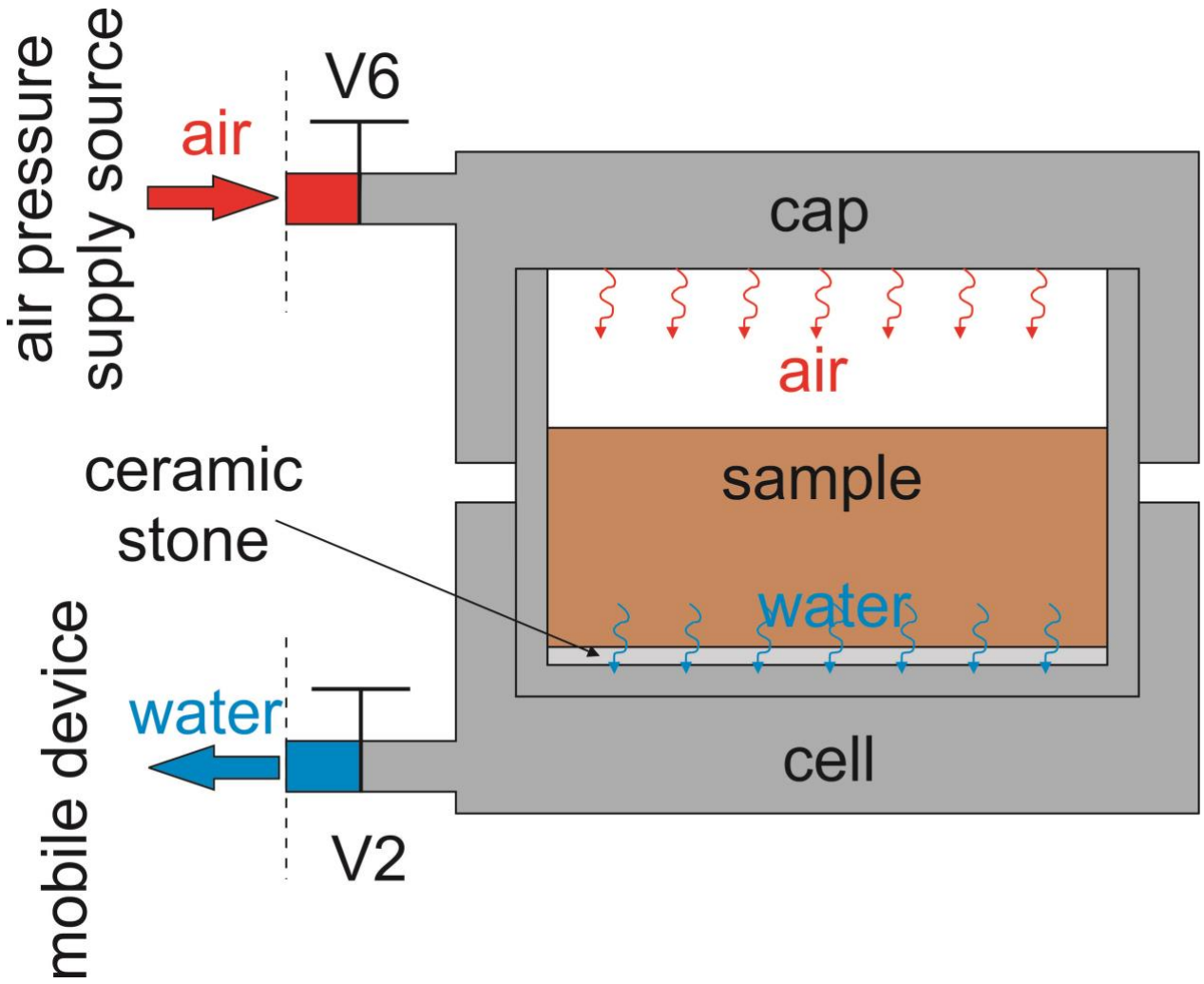

Figure 6. Application of the axis translation technique

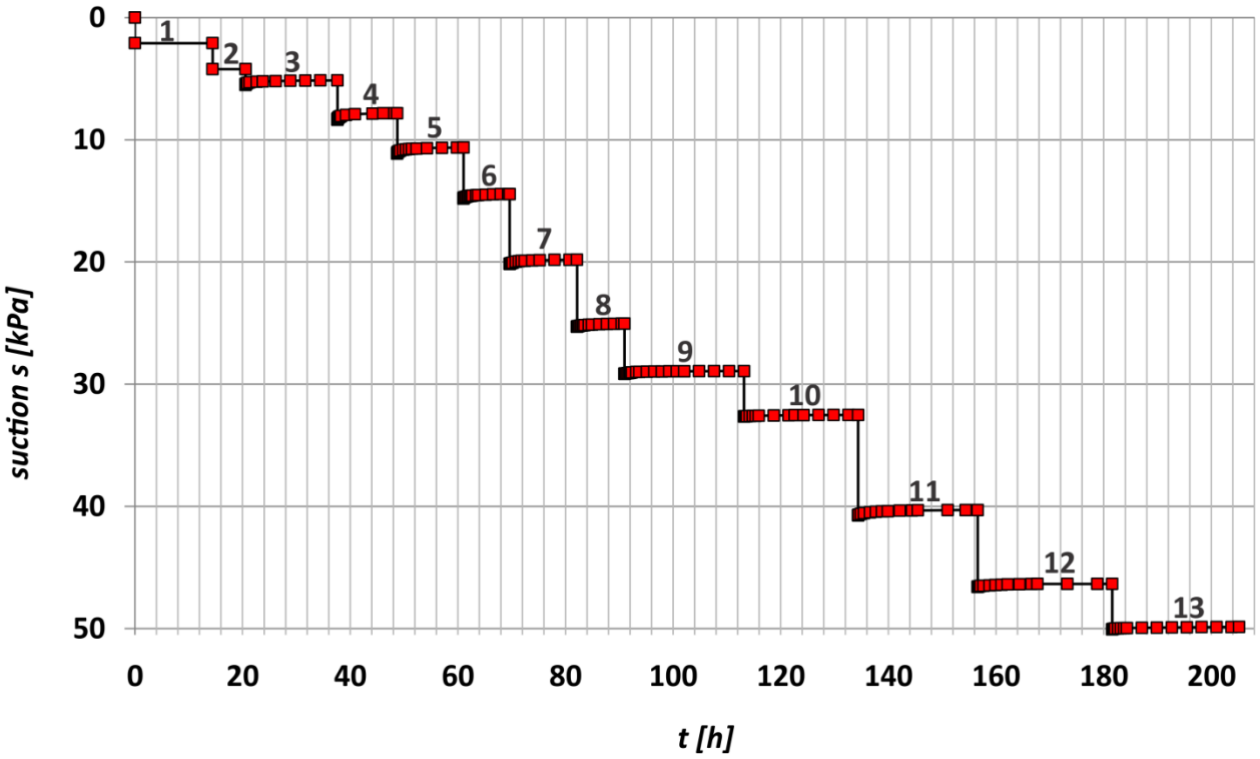

Figure 7. Continuous monitoring of the imposed suctions during the 13 steps, provided by the differential pressure transducer.

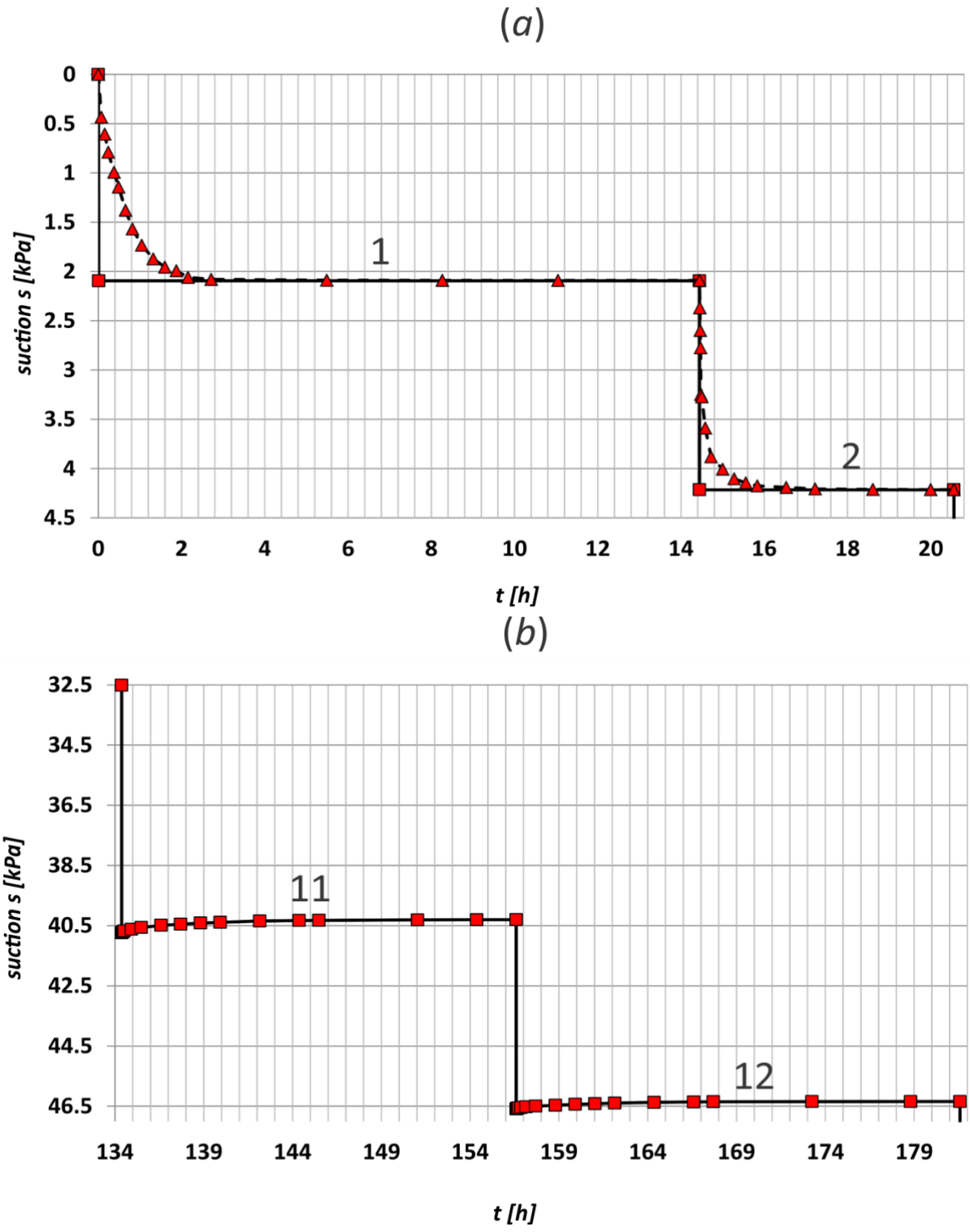

660

661 *Figure 8.* Zoom of the suction changes (solid line with rectangles – imposed suction; dashed line

662 with triangles – calculated suction at the top of the ceramic disk): a) steps 1 and 2; b) steps 11 and

663 12

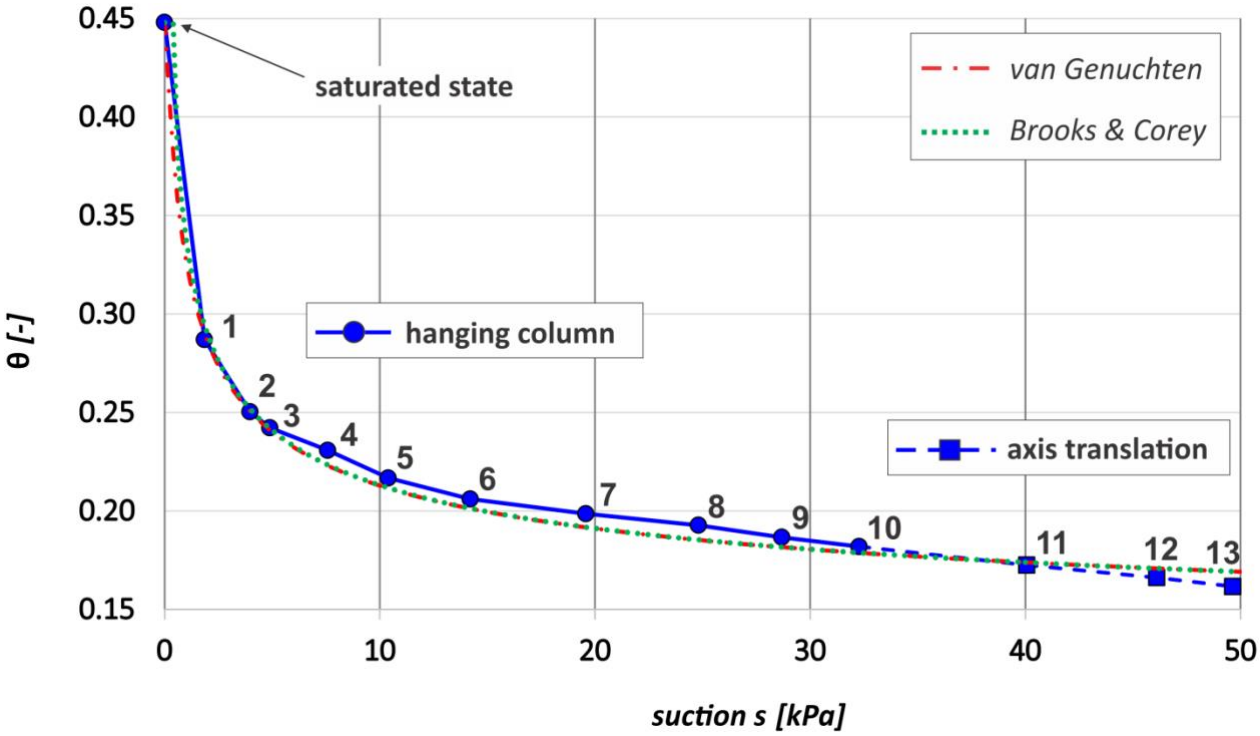

Figure 9. Water retention curve obtained using both techniques of controlling suction (hanging column and axis translation)

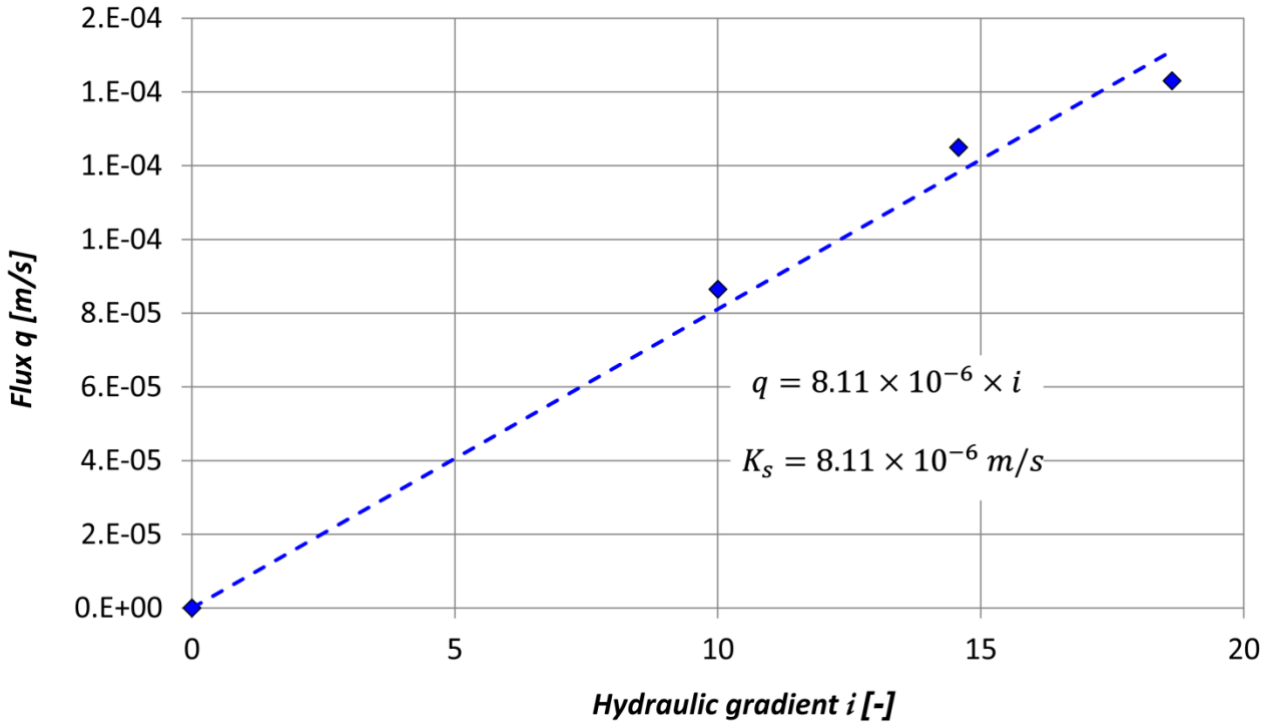

Figure 10. Data of the constant water head hydraulic conductivity measurement of the saturated material.

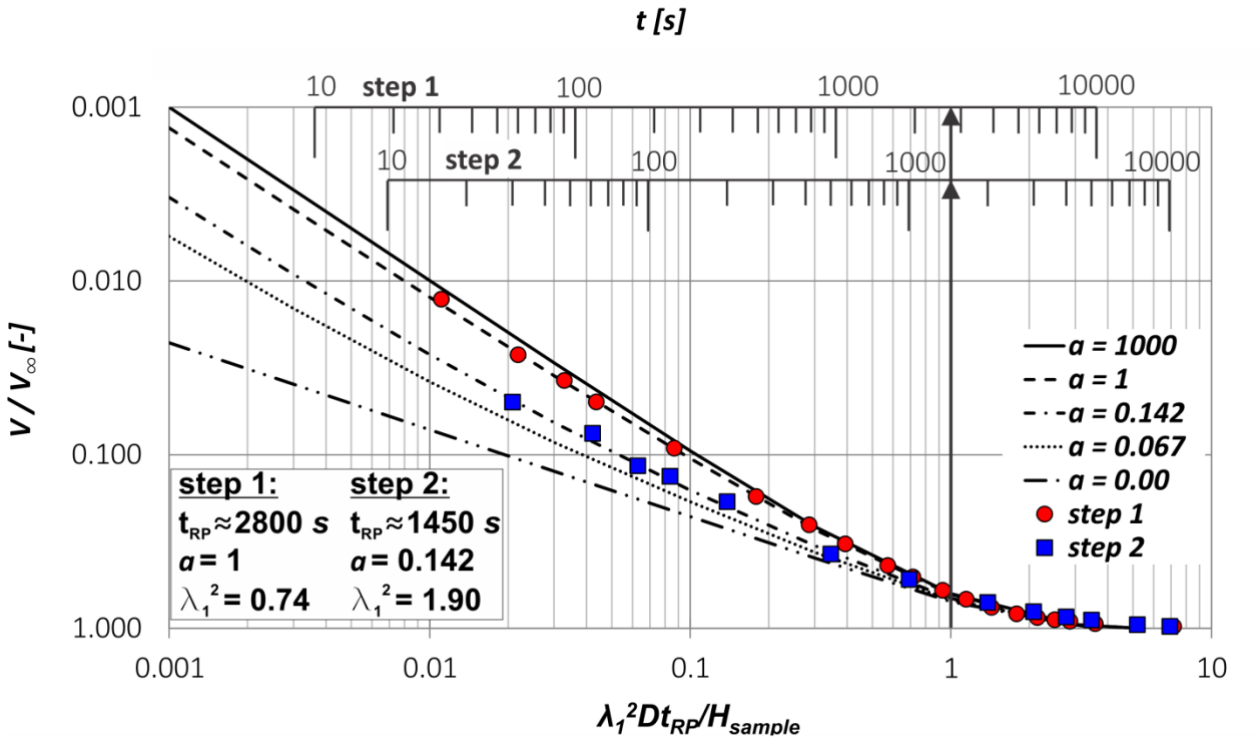

691

692 *Figure 11. Kunze and Kirkham's method applied to measurements 1 and 2 (arrow indicates t_{RP})*

693

694

695

696

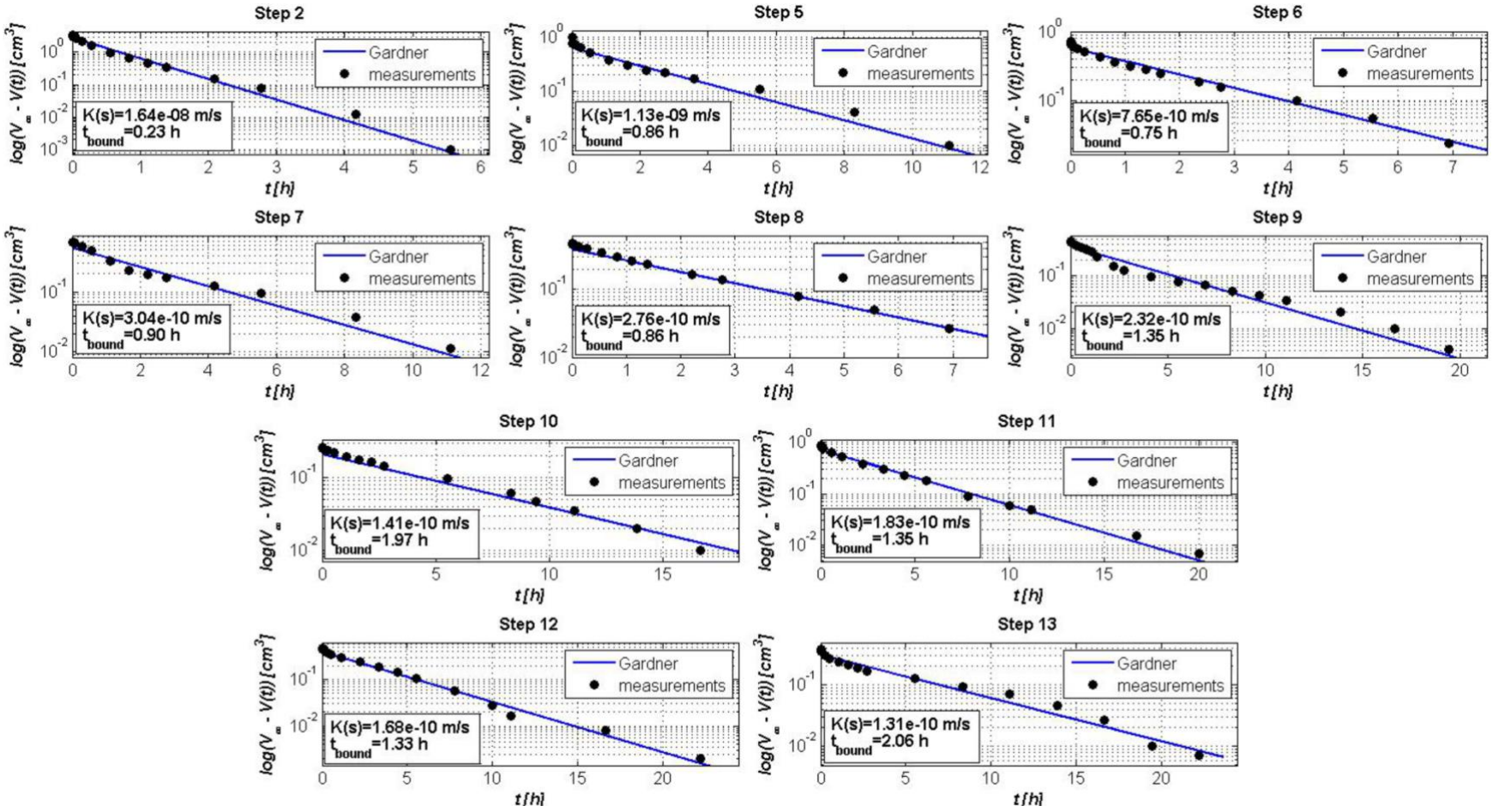

Figure 12. Data from Gardner's method, suction steps 2 and 5 – 13

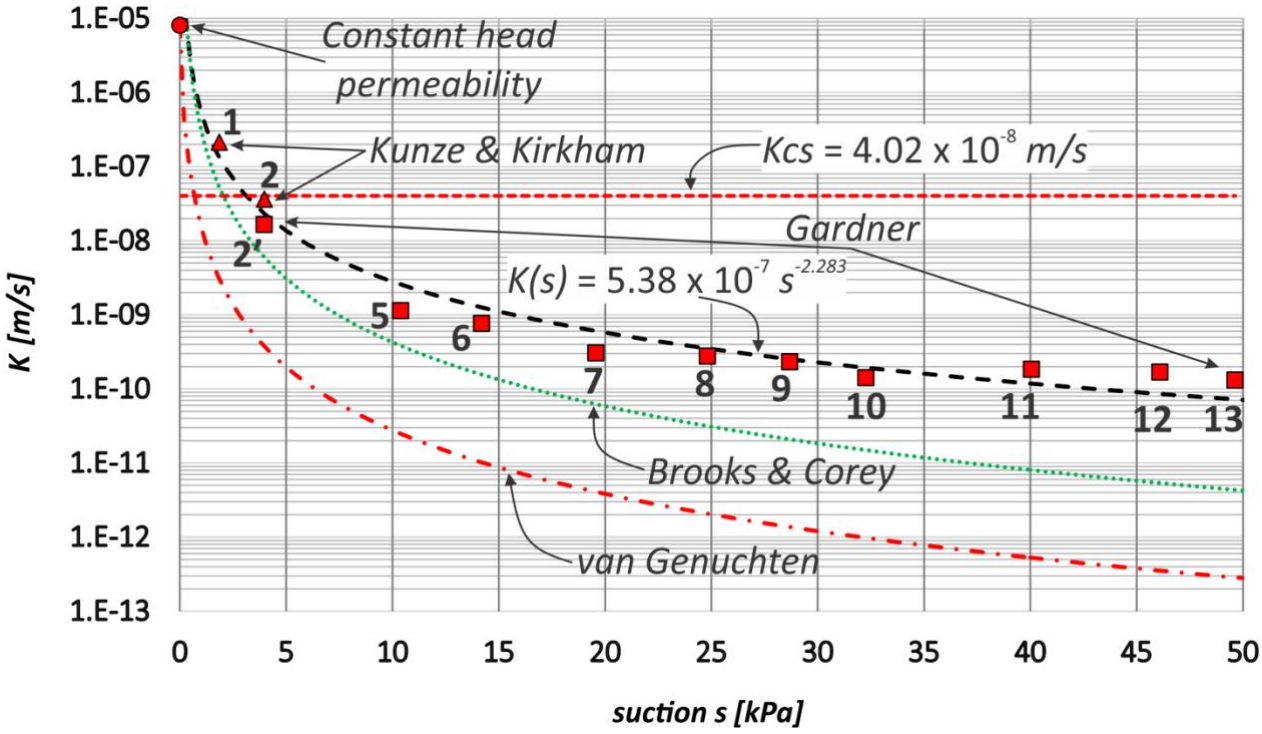

700

701 *Figure 13. Hydraulic conductivity function (HCF)*

702